مجموعه مقالات سومین کنفرانس ملی مهندسی مخازن هیدروکربوری و صنایع بالادستی
تهران، ۲۹ خرداد ماه ۱۳۹۳ مجری: هم اندیشان انرژی کیمیا
www.Reservoir.ir تلفن: ۸۸۶۷۱۶۷۶ - ۰۲۱

SIMULATION OF LARGE-SCALE HETEROGENEOUS FRACTURED BLOCKS

KHOSRO RAHIMI [1]–HOMA RAHIMI [2]–EHSAN SHAHBAZI [3]
(1) Science and Research branch, Islamic Azad University, Petroleum Department

*Correspondence author: Email: KHR.RAHIMI@GMAIL.COM

ABSTRACT

In this paper, we perform dynamic imbibition simulations on a large scale heterogeneous fractured block. The purpose is to seek optimum conditions under which maximum oil can be recovered in large-scale extremely-heterogeneous reservoirs. In this paper, we only consider horizontal wells. However, we simulate both continuous and slug injection scenarios. Various chemical solutions are injected. These include: water, polymer, surfactant, alkali, and different combinations of them. For convenience of simulation, although this is not physically correct, alkali represents the wettability modifying agent, while the surfactant is the agent that lowers the IFT to ultra-low values. Therefore, a simulation labeled AS indicates that the injected chemical solution lowers the IFT to ultra low values as well as alters the wettability from mixed-wet to water-wet. On the other hand, a simulation labeled ASP does the above task as well as making the chemical solution viscous (polymer). The recovery curves are compared and appropriate profiles are demonstrated in order to understand the results.

KEYWORDS: Chemical-enhanced , ASP flood, Surfactant, Static ,Dynamic .Imbibition Test.

[1] M.Sc. Student
[2]Sc. Student
[3]M.Sc. Student

1. MODEL DESCRIPTION

The Simulation model is a large-scale extremely-heterogeneous fractured block and is shown in Figure .1.

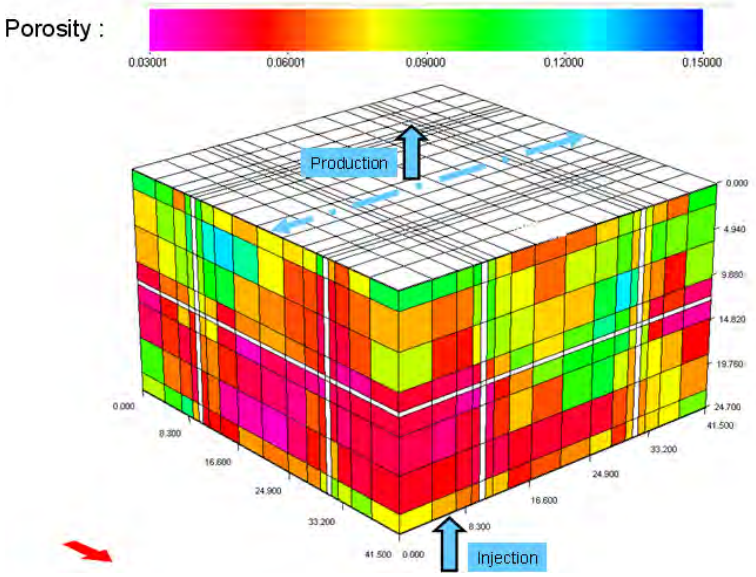

Figure .1 - Reservoir model for the large-scale heterogeneous fractured block simulations

This figure illustrates the distribution of the porosity. The white grid blocks indicate fractures. This is a 41.5 ft by 41.5 ft by 24.7 ft fractured block modeled with UTCHEM. There are 18 grid bocks in the X direction, 18 grid blocks in the Y direction and 11 grid blocks in the Z direction. The fractures are modeled as discrete fractures. There are two vertical fractures along the X axis and two vertical fractures along the Y axis. There are also three horizontal fractures perpendicular to the Z axis. As shown in the figure, one of these three horizontal fractures contains the injection well (at the bottom), one is in the middle and the last one contains the production well (at the top). The production well is shown by the blue array at the top of the block. The injection well has exactly the same orientation but is located under the block. Because the height of this fractured block is 24.7 ft and the wells are horizontal, buoyancy is should play a role here. The top, bottom and sides of the block are sealed. The block matrix is extremely heterogeneous with a Dykstra-Parson coefficient of 0.95. The values for matrix permeability were generated using the FFT program. The porosities were then generated from the permeablities according to the following correlation:

$$\phi = \left(\frac{k}{2*10^9} \right)^{1/8}$$

Where k has a unit of md. The block physical properties are listed in Table .1. The initial water saturation is 0.2 in the matrix and 0.99 in the fracture. Initially the matrix is mixed-wet. The capillary pressure in the fracture is always zero.[1-7] The capillary pressure for the matrix is calculated using the Brook-Corey model. The relative permeability parameters are calculated. In current paper, in all cases where surfactant is involved, surfactant forms a type III microemulsion with oil. Alkali, when present, changes the wettability with a constant value

of ω = 0.5 This is an approximation, but it has been found to be convenient to match the experimental data. The Initial condition parameters together with rock and fluid properties are listed in Table .2. The word "altered", wherever seen in this table, represents the value of the same parameter in a completely water-wet condition.

Block Length	41.5 ft
Block Width	41.5 ft
Block thickness	24.7 ft
Matrix size	(4,3,2,1,0.75) ft by (4,3,2,1,0.75) ft by (4,2,0.1) ft
Fracture spacing	20 ft in X and Y direction
Fracture aperture	0.75 ft for vertical and 0.5 ft for horizontal fractures
Average matrix porosity	0.075
Dykstra-Parson coefficient	0.95
Min and max matrix porosities	0.03 and 0.18
Average matrix permeability	13.15 md
Min and max matrix permabilities	0.0013 md and 2077 md
Fracture porosity	1
Fracture permeability	10000 md
Total effective permeability	1000 md
Total Fracture Porosity	50%
Block dip angle	0

Table .1 - Physical properties for the large-scale heterogeneous fractured block

Number of phases in the reservoir	Up to 3: water, oil, and microemulsion
Residual water saturation in matrix at low capillary number	0.1 , altered: 0.2
Residual water saturation in fracture at low	0.05 , altered: 0.1

capillary number	
Initial water saturation in matrix	0.2
Initial water saturation in fracture	0.99
Residual oil saturation in matrix at low capillary number	0.4, altered: 0.2
Residual oil saturation in fracture at low capillary number	0.15, altered: 0.05
Initial oil saturation in matrix	0.8
Initial oil saturation in fracture	0.01
Residual microemulsion saturation in matrix at low capillary number	0.1 , altered: 0.2
Residual microemulsion saturation in fracture at low capillary number	0.05, altered: 0.1
Residual saturation of all phases at high capillary number	0
Endpoint relative permeability of water at low capillary number	0.3 (altered: 0.2) for matrix, 0.4 (altered: 0.3) for fracture
Endpoint relative permeability of oil at low capillary number	0.4 (altered: 0.7) for matrix, 0.6 (altered: 1) for fracture
Endpoint relative permeability of microemulsion at low capillary number	0.3 for matrix (altered: 0.2), 0.4 (altered: 0.3) for fracture
Relative permeability exponent of aqueous phase at low capillary number	2 for matrix (altered: 2.5), 1.5 (altered: 2) for fracture
Relative permeability exponent of oil phase at low capillary number	3 for matrix (altered: 2), 1.8 (altered: 1.5) for fracture
Relative permeability exponent of microemulsion phase at low capillary number	2 for matrix (altered: 2.5), 1.5 (altered: 2) for fracture
Endpoint relative permeability of all phases at high capillary number	1
Relative permeability exponent of all phases at high capillary number	1
Matrix positive capillary Pressure Endpoint	variable (see Table 6.5 and 6.6)

Matrix negative capillary Pressure Endpoint	variable (see Table 6.5 and 6.6)
Matrix capillary pressure parameter EPC0	3 (altered: 3)
Matrix critical water saturation SSTAR (transition saturation from Pc+ to Pc-)	0.41 (altered: N/A)
Wettability alteration parameter	ω = constant = 0.5
Molecular diffusion coefficients of all components	0
Dispersivity of all phases	0
Surfactant adsorption parameters	AD31: 1.5, AD32: 0.15, B3D:1000
Polymer Viscosity parameters	
Polymer Permeability reduction parameter	CRK=0.12
Cation Exchange	N/A
Water viscosity	1 cp
Oil viscosity	10 cp
Microemulsion viscosity parameters	ALPHAV1 = 2.5 ALPHAV2 = 2.45 ALPHSV3-5 = 0
CMC	0.0005
Lower type III effective salinity	0.77
Higher type III effective salinity	1.15
Initial reservoir effective salinity for continuous-injection	0.82
Initial reservoir effective salinity for slug-injection	1.3
Slug effective salinity	0.95
Polymer-drive effective salinity	0.6

Table .2 - Rock and fluid properties for the large-scale heterogeneous fractured block

Eight different chemicals are injected: water only (W), surfactant only (S), alkaline only (A), polymer only (P), alkaline-surfactant (AS), alkaline-polymer (AP), surfactant- polymer (SP), and alkaline-surfactant-polymer (ASP). The injection and production wells are horizontal, constrained to constant pressures and completed in the lowermost and uppermost fractures, respectively. The well data are listed in Table .3.

Number of Injectors	1

Number of producers	1
Distance between injector and producer	48.5 ft
Perforation grids for injector	(9, 1-18, 1)
Perforation grids for producer	(9, 1-18, 11)
Producer BHP	14.7 psi
Injector BHP	Variable (see Table 6.5 and 6.6)
Constraint on injector or producer	Unlimited injection or production rates
Injected surfactant concentration, If any	2%
Injected alkali concentration, If any	1
Injected polymer concentration, If any	0.1 wt% for continuous-injection variable for slug-injection (Table 6.6)
Injected salinity	0.95 (inducing phase III microemulsion)
Chemicals injected	W, S, P, A, AS, SP, AP, ASP for continuous-injection ASP, AP for slug-injection

Table .3 - Well data for the large-scale heterogeneous fractured block

This model contains 3564 grid blocks, 1516 of which are fracture grid blocks. The total simulation time is 3 pore volumes. The UTCHEM solves the equations using the IMPES technique. The simulation parameters are listed in Table .4.

Total number of grid blocks	3564
Total number of fracture grid blocks	1516
Method of solution	IMPES
Simulation time	3 pore volumes

Table .4- Simulation data for the large-scale heterogeneous fractured block

The study cases are described in the upcoming sections.[8-12]

2. CONTINUOUS-INJECTION CASE STUDIES AND RESULTS

Two case studies for continuous injection are considered (Table .5). One case has a high pressure drop of 1 psi/ft and a low capillary pressure while the other one has a low pressure drop of 0.5 psi/ft and a higher capillary pressure. It should be noted that the chemicals are injected against the gravity direction (from bottom to top) and therefore the effective pressure drop will be much lower for each study case compared to what is stated in Table .5.

Case #	Pressure drop (psi/ft)	positive capillary pressure endpoint	negative capillary pressure endpoint
1	1	5	-5
2	0.5	10	-10

Table .5 - Case studies - Continuous-injection

Different chemicals are injected in each case: W, S, P, A, AS, SP, AP and ASP.
The oil recovery curves for the first case and the second case are depicted in Figures .2- .3 and .4- .5, respectively.

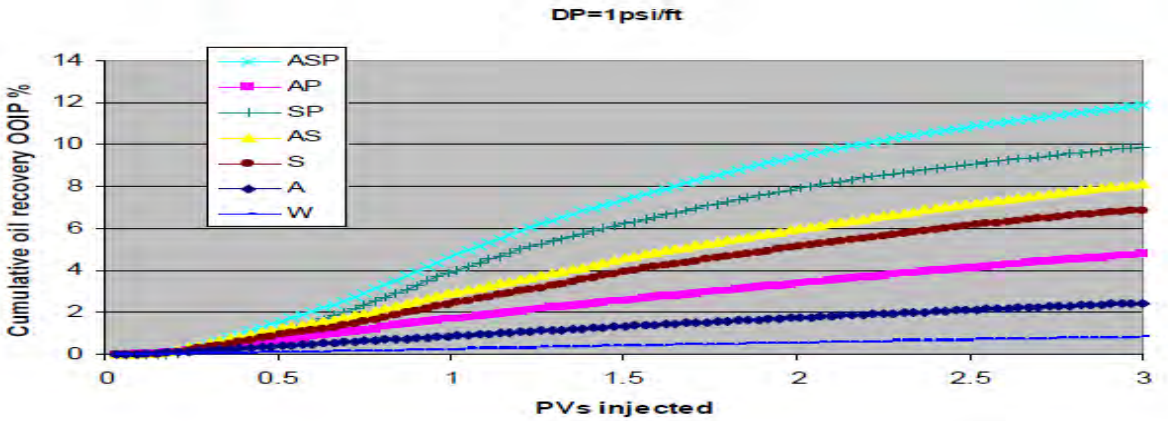

Figure .2 - Comparing oil recovery versus PV for different chemicals, DP=1psi/ft

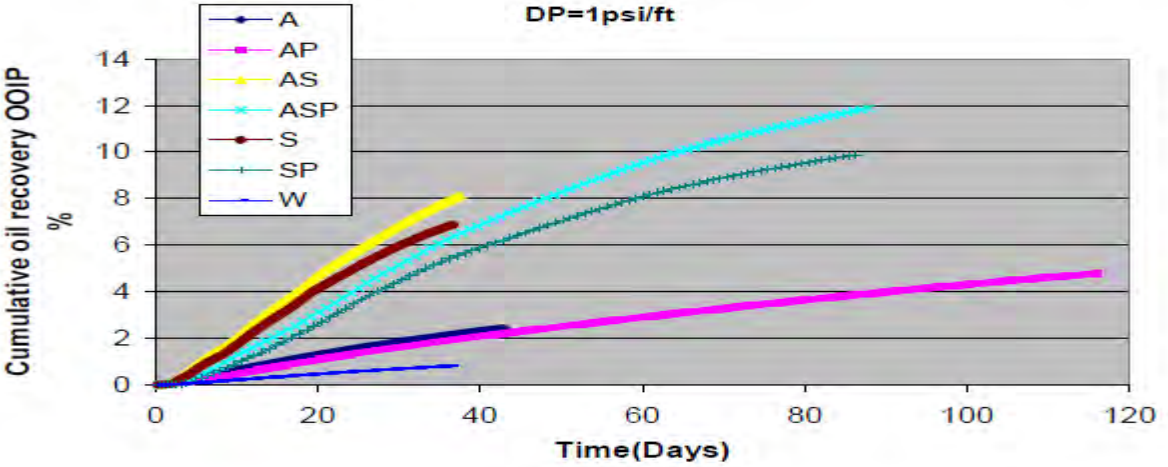

Figure .3 - Comparing oil recovery versus time for different chemicals, DP=1psi/ft

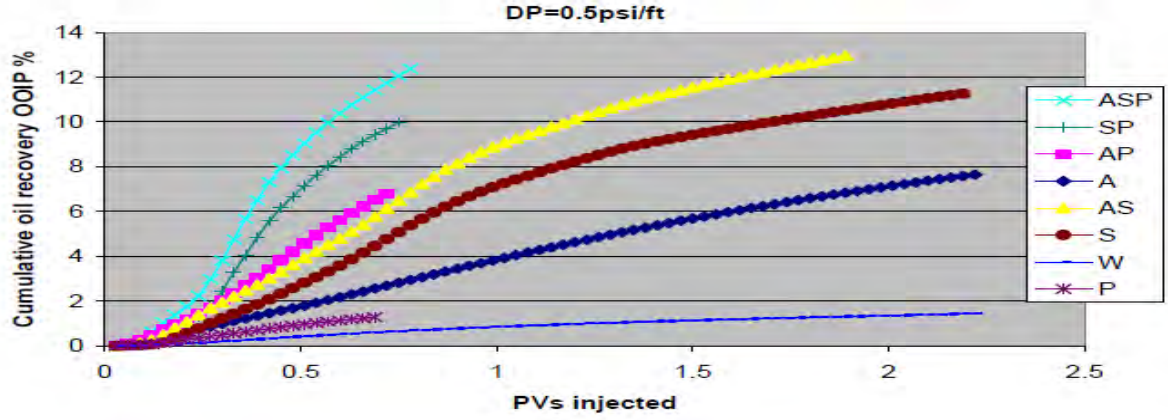

Figure .4 - Comparing oil recovery versus PV for different chemicals, DP=0.5 psi/ft

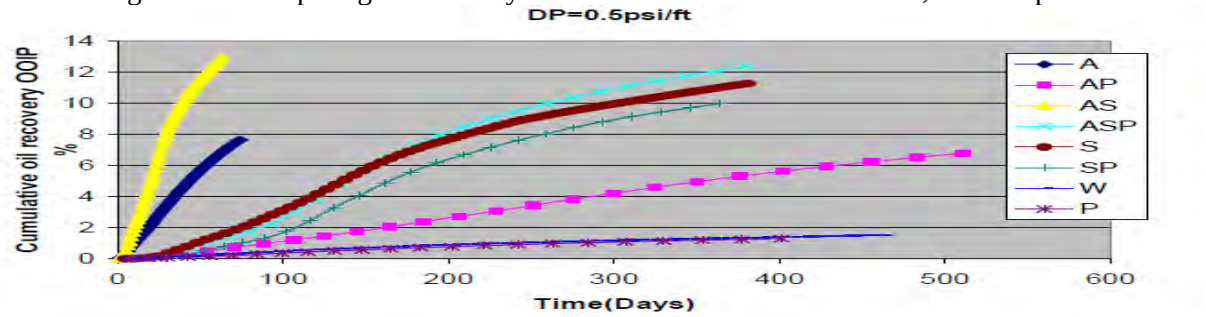

Figure .5 - Comparing oil recovery versus time for different chemicals, DP=0.5 psi/ft

Figure .2 and .4 show the oil recovery versus PVs while Figures .3 and .5 show the oil recovery versus time. By looking at Figures .2 and .4, we observe that ASP flooding results in the highest and fastest oil recovery. This result is therefore independent of how high or low the contrast between the capillarity and viscous forces is. The second highest oil recovery goes to SP flooding. In both Figures, alkaline flooding is inferior to surfactant flooding. In contrast, Figures .3 and .5 reveal that AS flooding has the best performance when oil recovery is compared versus time. The second best performance goes to surfactant flooding in Figure .3 and alkaline flooding in Figure .5. This seems reasonable as capillarity is dominant in Figure .5 whereas viscous forces are dominant in Figure .3. The superiority of AS flooding in Figures .3 and .5 shows that lowering the IFT to ultra-low values, and altering the wettability at the same time produce the best result. The reason that AS is inferior to ASP, when analyzing the recoveries versus time, is only because the polymer reduces the injection rate (in our fixed pressure simulations).

3. SLUG-INJECTION CASE STUDIES AND RESULTS

These final series of simulations determine what the optimal conditions should be in order to produce the maximum amount of oil, when injecting a chemical solution into a heterogeneous fractured reservoir. Nine cases for slug injection are considered (Table .6). All cases include a chemical slug size of between 0.3 and 0.5 pore volumes. The chemical slug is, in all cases, followed by a continuous slug of polymer until a total of three pore volumes have been injected. In all cases, the chemical slug includes polymer as well. The concentration of the polymer in the chemical slug is always equal to that of the polymer drive. Additionally, there is always a salinity gradient established between the initial reservoir salinity, slug salinity and polymer-drive salinity (Table .2). Cases 1-6 investigate the effect of slug-size and polymer concentration on the recovery. On the other hand, Cases 7-9, when compared with cases 1-3, evaluate the effect of the reduced pressure gradient and the increased capillary pressure. It should be noted that the chemicals are injected against the gravity direction (from bottom to top) and therefore the effective pressure drop will be much lower for each study case compared to what is stated in Table .6.

Case #	Pressure drop (psi/ft)	Slug size (PV)	Polymer concentration in surfactant slug (=surfactant concentration in drive slug) (wt %)	positive capillary pressure endpoint	negative capillary pressure endpoint
1	1	0.3	0.1	5	-5
2	1	0.4	0.1	5	-5
3	1	0.5	0.1	5	-5
4	1	0.3	0.2	5	-5
5	1	0.4	0.2	5	-5
6	1	0.5	0.2	5	-5
7	0.5	0.3	0.1	10	-10
8	0.5	0.4	0.1	10	-10
9	0.5	0.5	0.1	10	-10

Table .6 - Case studies - Slug-injection

The injected chemicals in this section are ASP and AP only. Hence, we will be able to determine which chemical produces a better result in terms of a faster and higher ultimate recovery.

In the case of ASP flooding, Figure .6

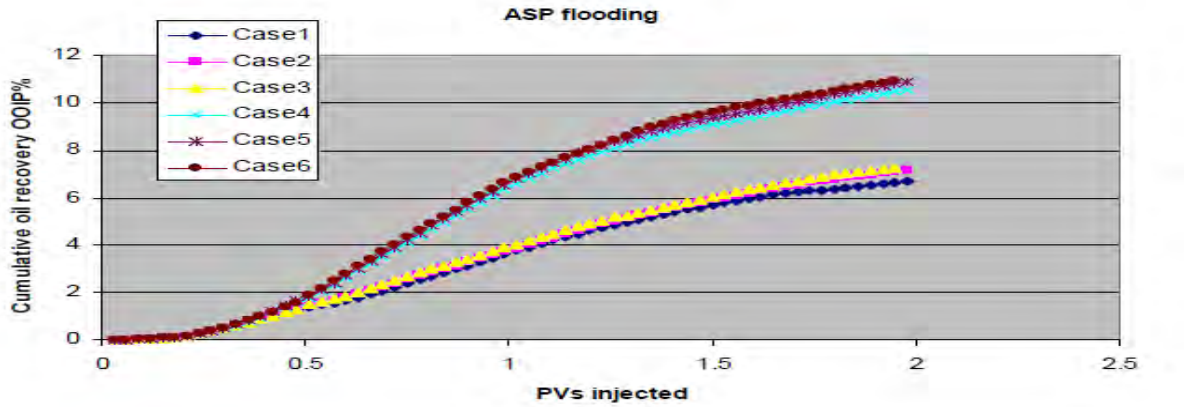

Figure .6 - Comparing oil recoveries for ASP flooding, Cases 1-6

shows that increasing the polymer concentration from 0.1 wt% to 0.2 wt%, drastically enhances the oil recovery versus pore volumes injected. The ultimate oil recovery is around 11% for a polymer concentration of 0.2 wt% (cases 1-3) whereas 7% (cases 4-6) for a polymer concentration of 0.1 wt%. This is because of the increased sweep efficiency and the greater transverse pressure gradients. On the other hand, the effect of slug size on oil recovery is very small. The reason is that most of the injected chemicals are transported through the fractures (where there is no matrix rock) and therefore the surfactant adsorption is small. Another reason is that a value of zero has been assigned to diffusion and dispersion coefficients in these simulations. Consequently the dilution of the chemical slug should be insignificant.

In the case of AP flooding, Figure .7

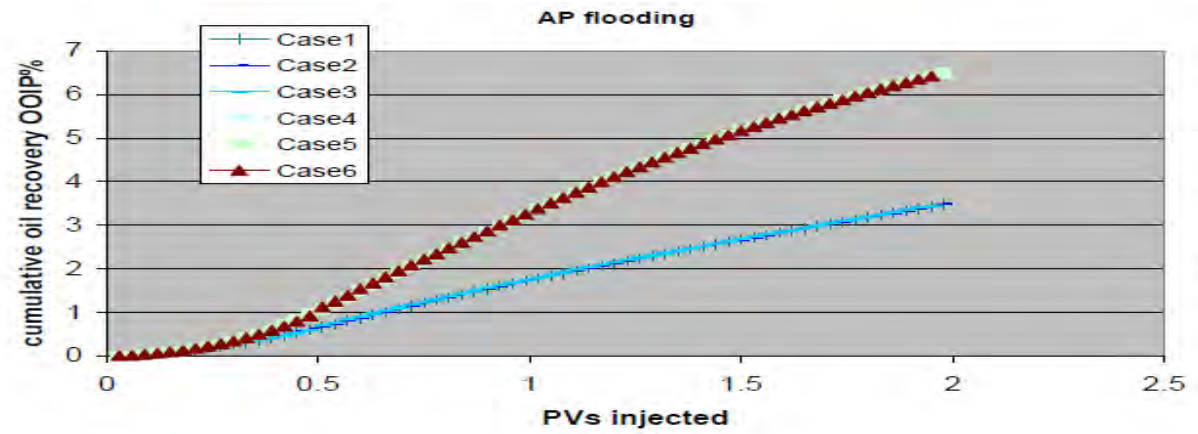

Figure .7 - Comparing oil recoveries for AP flooding, Cases 1-6

shows the same effect of increasing the polymer concentration from 0.1 wt% to 0.2 wt%, as in the case of ASP flooding. For these simulations, however, the adsorption parameter for the chemical has been set to zero. The result of doing so was that the slug size did not affect the recovery curves at all. This result confirms that dilution and adsorption are the two reasons for loss of a chemical slug.

Figure .8 summarizes the results of the simulations for cases 1-6 and compares their oil recoveries versus days.

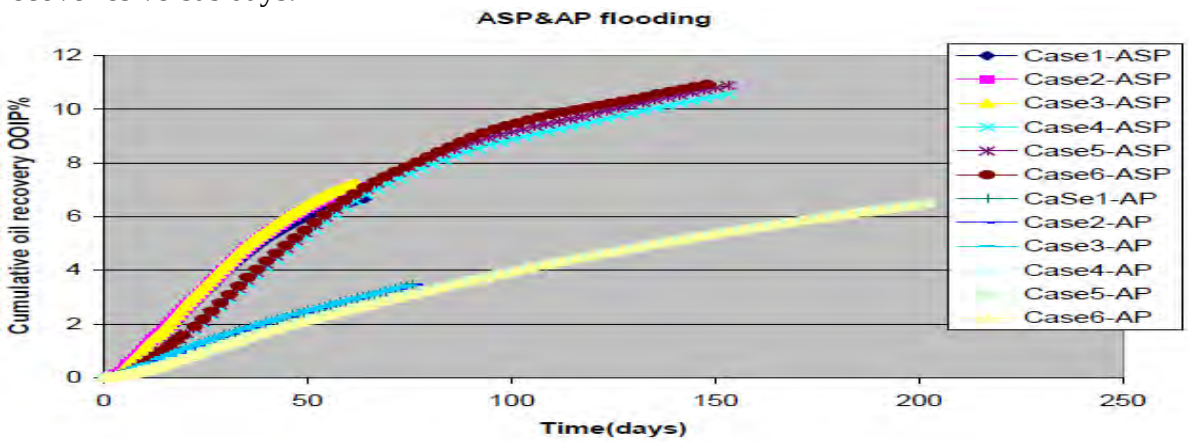

Figure .8 - Comparing oil recoveries for ASP & AP flooding, Cases 1-6

We can observe that ASP flooding is absolutely superior to AP flooding even when the recoveries are compared on a time basis. Additionally, we can deduce that increasing the polymer concentration from 0.1 wt% to 0.2 %, results in a much higher ultimate oil recovery, although the recovery curve starts off slower. This is consistent in both ASP and AP flooding cases.

Finally, Figures .9 and .10

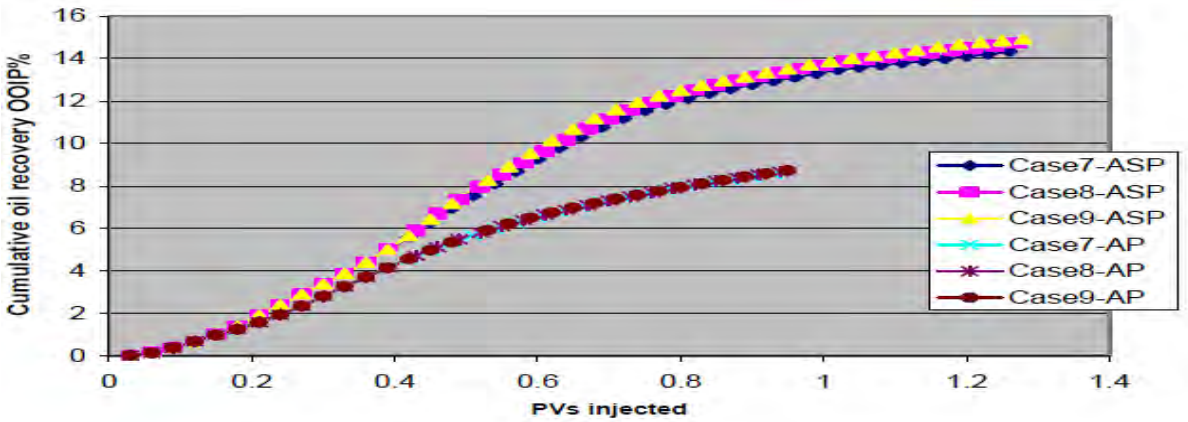

Figure .9 - Comparing oil recovery versus PV for ASP & AP flooding, cases 7-9

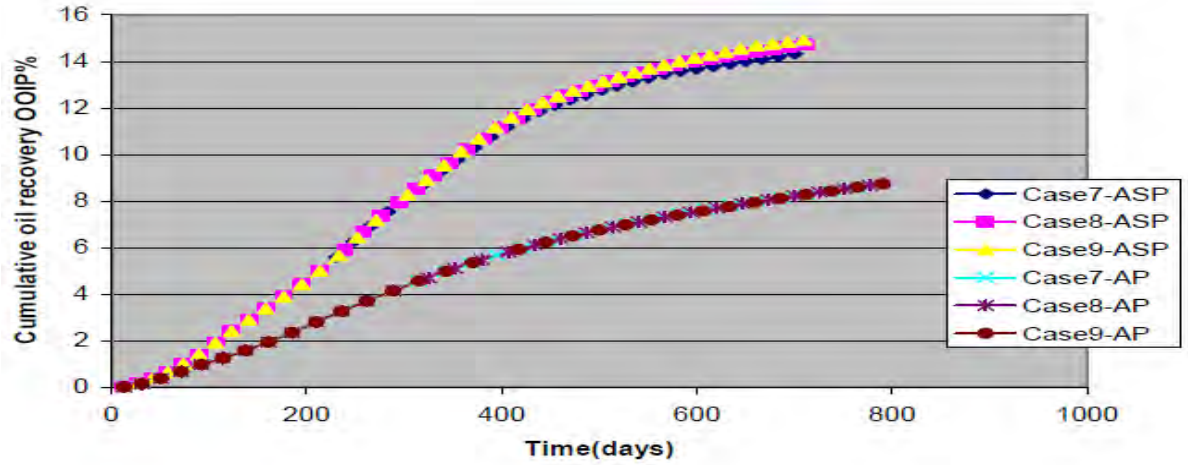

Figure .10 - Comparing oil recovery versus time for ASP & AP flooding, cases 7-9

depict the recovery curves for cases 7-9 and versus pore volumes and day, respectively. We observe that ASP flooding still outperforms AP flooding and this is irrespective of what the time basis is (PV or day). Comparing the Figure .9, together with Figures .6 and .8, reveal that cases 7-9 yield a much higher oil recovery compared to those of cases 1-3. This is mainly because of the reduced pressure drop and consequently the increased contact time. The slug size effect is again insignificant for the reason previously mentioned.

REFERENCES

1. Anderson, J.L., Eyring, E.M., and Whittaker, M.P. 1964. Temperature Jump Rate Studies of Polyborate Formation in Aqueous Boric Acid.The Journal of Physical Chemistry 68 (5): 1128-1132. doi: 10.1021/ j100787a027.
2. Aoudia, M., Wade, W.H., and Weerasooriya, V. 1995. Optimum microemulsions formulated with propoxylated tridecyl alcohol sodium sulfates.Journal of Dispersion Science and Technology 16 (2): 115-135. doi:10.1080/01932699508943664.
3. Austad, T. and Milter, J. 2000. Surfactant Flooding in Enhanced Oil Recovery. In Surfactants: Fundamentals and Applications in the Petroleum Industry, ed. L.L. Schramm, Chap. 6, 203-249. Cambridge, UK: Cambridge University Press.
4. Bhuyan, D. 1989. Development of an Alkaline/Surfactant/Polymer Compositional Reservoir Simulator. PhD dissertation, University of Texas,Austin, Texas, USA.

5. Bhuyan, D., Lake, L.W., and Pope, G.A. 1991. Simulation of High-pH Coreflood Experiments Using a Compositional Chemical Flood Simulator. Paper SPE 21029 presented at the SPE International Symposium on Oilfield Chemistry, Anaheim, California, USA, 20-22 February. doi: 10.2118/21029-MS.
6. Bunge, A.L. and Radke, C.J. 1983. Divalent Ion Exchange With Alkali. SPE J. 23 (4): 657-668. SPE-8995-PA. doi: 10.2118/8995-PA.
7. Wang, W., Gu, Y., and Liu, Y.:"Applications of Weak Gel for In-Depth Profile Modification and Oil Displacement," J.Cdn. Pet. Tech.(June 2003) 42, 54.
8. Arihara, N. et al.: "Oil Recovery Mechanisms of Alkaline-Surfactant-Polymer Flooding," paper SPE 54330 presented at the 1999 SPE Asia Pacific Oil and Gas Conference and Exhibition, Jakarta, 20-22 April.
9. Wang, D., Zhang, Z., Chen, J., Yang, J., and Go, S.,Pilot Tests of Alkaline/Surfactant/Polymer Flooding in Daqing Oil Field," SPE Reservoir Engineering, (Nov. 1997) 229-233.
10. Dong, M and Huang, S.,"Potential ofAlkaline/Surfactant/Polymer (ASP) Flooding of Southwest Saskatchewan Medium Oil Reservoirs", CIPC paper No. 2002-109 present at the Petroleum Society's Canadian International Petroleum Conference 2002, Calgary, Alberta, Canada, June 11-13, 2002.
11. Adibhatla, B. & Mohanty, K.K. 2008. Oil Recovery from Fractured Carbonates by Surfactant Aided Gravity Drainage:Laboratory Experiments and Mechanistic Simulations. SPE Res Eval & Eng,11(1):119130. SPE 99773-PA. doi:10.2118/99773-PA
12. Barnes, J.R., Smit, J.P., Smit, J.R., Shpakoff, P.G., Raney, K.H., Puerto, M.C. 2008. Development of Surfactants for Chemical Flooding at Difficult Reservoir Conditions. Paper presented at the SPE/DOE Symposium on Improved Oil Recovery, Tulsa, Oklahoma, 20-23 April. doi: 10.2118/113313-MS